

# Analysis of Influence of Moving Axial Load on Elevated Box Bridge of Slab Track

Xiaoyun Zhang, Guangtian Shi<sup>(✉)</sup>, Xiaoan Zhang, and Yanliang Cui

School of Mechanical Engineering, Lanzhou Jiaotong University,  
Lanzhou 730070, China  
zxa\_lzjtu@163.com

**Abstract.** Due to the increasingly usage of the heavy-load train, the effect of the moving axial load on the noise radiation of elevated bridge structure should be concerned. In this paper, high speed train-track-bridge coupled model is established, and the train axle load, which is taken as the boundary condition of the load, is applied to the finite element model of elevated box bridge structure to calculate the vibration response of the surface of a box bridge. In this model, the vibration response is taken as the acoustic boundary conditions and is added to the boundary element model of elevated box bridge structure to study its sound radiation. The results show that the plate-shell unit can well reflect the overall and local vibration characteristics of the bridge structure, and under the effect of moving axial load, the vibration frequencies of box bridge structure concentrate in 0–300 Hz and the main peaks are in 10–160 Hz; the finite element-boundary element method can effectively analyze the low frequency noise radiation of box bridge caused by the moving axial load; the most of structure noise induced by moving axial load is below the audible range of which the noise is greatly harmful to human body, thus it must be taken seriously.

**Keywords:** High speed railway · Elevated box bridge · Moving axial load · Finite element-boundary element method · Sound radiation

## 1 Introduction

For dynamic interaction of railway system and structure noise, in early researches, Zhai W.M. et al. analyzed the dynamic mechanism between the locomotive and the track structure of the high-speed trains through the bridge. On this basis, train-track-bridge coupled model was established, and then being validated and analyzed based on the field measurements of Qinhuangdao-Shenyang Passenger Dedicated Line. The dynamic characteristics of the high-speed trains passing through the bridge at different speeds are characterized by the compiled program TTBSIM [1–3]. He Z.X. et al. studied the ground vibration under the simple harmonic loads by semi-analytical method and analyzed the energy transfer characteristics between the track, the foundation and the effect of the simple harmonic load on the vibration attenuation. The ground vibration caused by the train axial load and its propagation characteristics and the vibration damping effect of the isolation groove are simulated and analyzed [4, 5].

Thompson et al. made extensive researches on the vibration and control of railway noise and developed the corresponding software to guide the low noise and vibration design of train-track systems and noise reduction of the existing tracks [6–8]. Li X.Z. proposed a method for full-band noise prediction of high-speed railway bridge structures, a span of 32 m double-line simply supported concrete box bridge are regarded as the case study, and the field test and simulation analysis [9–11]. Augustinovicz F. et al. studied the structural noise of orthotropic box-bridge [12]. Ouelaa N. et al. calculated the acoustic pressure of the field, in which the three-span continuous bridge transient acceleration as the monopole excitation source is used by considering the coupling effect of vehicle-bridge and track irregularities and, taking only two degrees of freedom into account for each train [13]. Song et al. established the vertical coupling dynamic model of vehicle-track-elevated structure, and obtaining the force between the wheel-rails as the input of the statistical energy analysis to research on the vibration and acoustic radiation of elevated structure [14]. Ngai K.W. et al. proposed a vibration and noise test on a concrete box bridge of an elevated railway in Hong Kong. The results show that the noise and vibration frequency range of the elevated bridge is from 20 Hz to 157 Hz when the train runs at 140 km/h [15]. Li Qi et al. used the modal superposition method to calculate the train-track-bridge coupling dynamic of the urban rail transit trough girders, and calculating the structural noise of trough beam using the modal acoustic transmission vector and the modal coordinate response of the beam [16].

In this paper, the train axle load, taken as the load boundary conditions, is applied to the finite element model of elevated box bridge structure to calculate the vibration response of the surface of elevated box bridge. The vibration response of the box bridge structure is used as the acoustic boundary condition, and the noise radiation of elevated box bridge structure is analyzed by the Helmholtz boundary integral equation.

## 2 Noise Prediction Model of Elevated Box Bridge Under Axial Load

### 2.1 Train Axle Load

Generally, to the vehicle-track-bridge coupled system, the excitation sources of vibration mainly consist of two parts: the axle load and the dynamic loads induced by the track irregularities. When a train moves on the elevated bridge, the effects of the axle load on the vibrations of the bridge cannot be ignored because of the large size of the axle loads. It is therefore necessary to research the structural noise of the bridge originated from the axle loads. In this paper, the wheel-rail force is simplified as a series of axle loads while ignoring the influence of track irregularities, as shown in Fig. 1.

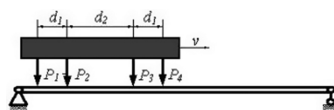


Fig. 1. The model of moving axle load on train

Assume the velocity of train is  $v$  and the wheel/rail vertical forces are  $p_1, p_2 \dots p_n$ , ( $n$  is the number of the wheels). The coordinate  $a_i$  ( $i = 1, 2, \dots n$ ) of each wheel is determined by  $d_1$  and  $d_2$  in Fig. 1. In the train operation, the force on track structure can be expressed as using Dirac-delta function (1).

$$P(t) = \sum_{j=1}^{N_w} \delta(x - vt - \alpha_j) p_j e^{\frac{2\pi v t}{\lambda} j} \tag{1}$$

### 2.2 The Equations of Motion and Solution

Because the axle loads directly act on the rail beams, the differential equation of motion of the rail can be described as

$$E_r I_r \frac{\partial^4 W_r(x, t)}{\partial x^4} + M_r \frac{\partial^2 W_r(x, t)}{\partial t^2} + C_{rs} \left[ \frac{\partial W_r(x, t)}{\partial t} - \frac{\partial W_s(x, t)}{\partial t} \right] + K_{rs} [W_r(x, t) - W_s(x, t)] \\ = - \sum_{i=1}^{N_s} F_{rvi}(t) \delta(x - x_{Fi}) + \sum_{j=1}^{N_w} \delta(x - ct - \alpha_j) p_j e^{\frac{2\pi v t}{\lambda} j} \tag{2}$$

Where,  $E_r$  and  $I_r$  denote the elasticity modulus and inertia moment of rail, respectively. The bending rigidity can be expressed as the product of elasticity modulus and inertia moment.  $M_r$  is the quality of each unit length of the rail.  $W_r, W_s$  denote the rail vertical displacement and the track vertical displacement.  $C_{rs}, K_{rs}$  denote the damping coefficient and stiffness coefficient connecting the rail and the track.  $N_s$  and  $N_w$  are the total number of the fastener and the wheel axle in the rails, respectively.  $F_{rvi}$  is the vertical reaction force of the  $i$ th supporting point of the rail.

The differential equation of motion of the track slab can be described as:

$$\frac{\partial^4 W_s(x, y, t)}{\partial x^4} + 2 \frac{\partial^4 W_s(x, y, t)}{\partial x^2 \partial y^2} + \frac{\partial^2 W_s(x, y, t)}{\partial y^4} + \frac{C_s}{D_s} \frac{\partial W_s(x, y, t)}{\partial t} + \frac{\rho_s h_s}{D_s} \frac{\partial^2 W_s(x, y, t)}{\partial t^2} \\ = \frac{1}{D_s} \left[ \sum_{i=1}^{N_p} P_{rvi}(t) \delta(x - x_{Pi}) \delta(y - y_{Pi}) - \sum_{j=1}^{N_f} F_{svj}(t) \delta(x - x_{Fj}) \delta(y - y_{Fj}) \right] \tag{3}$$

In the dynamic analysis of the bridge structures, the bridge system is divided as an assembly of shell element, and then selecting the shape functions to calculate the kinetic and potential energy of each unit, and consequently the entire structure. Finally, the dynamic equations of motion of the whole system can be derived by the Hamilton principle [1], which is

$$[M_b] \{\ddot{u}_b\} + [C_b] \{\dot{u}_b\} + [K_b] \{u_b\} = \sum_{j=1}^{N_f} F_{svj}(t) \delta(x - x_{Fj}) \delta(y - y_{Fj}) \tag{4}$$

Where,  $[M_b]$ ,  $[C_b]$  and  $[K_b]$  denote the mass matrix, damping matrix and stiffness matrix of the bridge;  $\{u_b\}$ ,  $\{\dot{u}_b\}$  and  $\{\ddot{u}_b\}$  denote the generalized vectors of displacement, velocity and acceleration of the bridge, respectively.

The Newmark method is used to calculate the dynamic response of the bridge by satisfying the following integral scheme.

$$\begin{cases} \{u_{n+1}\} = \{u_n\} + \{\dot{u}_n\}\Delta t + [(1/2 - \alpha)\{\ddot{u}_n\} + \alpha\{\ddot{u}_{n+1}\}]\Delta t^2 \\ \{\dot{u}_{n+1}\} = \{\dot{u}_n\} + [(1 - \beta)\{\ddot{u}_n\} + \beta\{\ddot{u}_{n+1}\}]\Delta t \end{cases} \quad (5)$$

The integral form is unconditionally stable if taking  $\alpha = 1/4$ ,  $\beta = 1/2$ . The time interval of the integration is 0.01 s. Use  $u_{n+1}$  to express  $\dot{u}_{n+1}$  and  $\ddot{u}_{n+1}$  in above formulas, and substitute them into the dynamic equations of the bridge system, that is,

$$[M_b]\{\ddot{u}_{b,n+1}\} + [C_b]\{\dot{u}_{b,n+1}\} + [K_b]\{u_{b,n+1}\} = \{F_{b,n+1}(t)\} \quad (6)$$

Therefore, the following equation can be obtained by resorting the above dynamic equation.

$$(a_0[M_b] + a_1[C_b] + [K_b])\{u_{b,n+1}\} = \{F_{b,n+1}(t)\} + [M_b](a_0\{u_{b,n}\} + a_2\{\dot{u}_{b,n}\} + a_3\{\ddot{u}_{b,n}\}) + [C_b](a_1\{u_{b,n}\} + a_4\{\dot{u}_{b,n}\} + a_5\{\ddot{u}_{b,n}\}) \quad (7)$$

With,  $a_0 = \frac{1}{\alpha\Delta t^2}$ ,  $a_1 = \frac{\beta}{\alpha\Delta t}$ ,  $a_2 = \frac{1}{\alpha\Delta t}$ ,  $a_3 = \frac{1}{2\alpha} - 1$ ,  $a_4 = \frac{\beta}{\alpha} - 1$ ,  $a_5 = \frac{\Delta t}{2}(\frac{\beta}{\alpha} - 2)$ .

The following formulas can be obtained by (5) and (7).

$$\begin{cases} \{\dot{u}_{b,n+1}\} = \{\dot{u}_{b,n}\} + a_6\{\ddot{u}_{b,n}\} + a_7\{\ddot{u}_{b,n+1}\} \\ \{\ddot{u}_{b,n+1}\} = a_0(\{u_{b,n+1}\} - \{u_{b,n}\}) - a_2\{\dot{u}_{b,n}\} - a_3\{\ddot{u}_{b,n}\} \end{cases} \quad (8)$$

With,  $a_6 = \Delta t(1 - \beta)$ ,  $a_7 = \beta\Delta t$ .

Therefore, the displacement, velocity and acceleration of the bridge system can be obtained.

### 2.3 Sound Field Solution

Because the dynamic responses of the box bridge are obtained in time domain, therefore, it is a necessity to transform the time-domain results into the frequency domain. Using the discrete Fourier transform, the responses of continuous frequency points can be obtained by the vibration responses of the box bridge structure in time domain. Then, we perform filtering on the results, that is, the time histories of the response can be obtained by the inversely discrete Fourier transform, and then calculating the root mean square (RMS) in every 1/3 octave band range as the outputs of the vibration response at 1/3 octave center frequency. The dynamic response of a node in directions toward different degrees of freedom can be projected to the normal direction of the structure, which is treated as the vibration boundary conditions of the structural element.

In the acoustic radiation of the closed structure in the fluid medium, the acoustic wave equation:  $\nabla^2 \vec{p} + k^2 \vec{p} = 0$ , the Neumann boundary condition of the fluid-solid interface:  $\frac{\partial \vec{p}}{\partial \vec{n}} = -i\rho_0 \omega \vec{v}_n$ , and the Sommerfeld radiation condition:  $\lim_{r \rightarrow \infty} \left[ r \left( \frac{\partial \vec{p}}{\partial r} - ik\vec{p} \right) \right] = 0$  must be satisfied.  $\nabla$ ,  $\vec{p}$ ,  $\omega$ ,  $c$ , and  $\rho_0$  represent the Laplacian operator, sound pressure, circular frequency, sound velocity and fluid density, respectively.  $i$  is the imaginary unit.  $k$  stands for wave number,  $k = \omega/c$ .  $\vec{v}_n$  is the normal velocity vector on the interface between the fluid and structure.  $r$  is distance between any point  $X$  on the structure surface  $Y$ ,  $r = |\vec{X} - \vec{Y}|$ .  $A$  is the surface area of the structure.

The Helmholtz integral equation can be obtained by the free space Green's formula,

$$C(Y)\vec{p}(Y) = \int_A (-i\omega\rho_0 \frac{e^{-ikr}}{4\pi r} \vec{v}_n(X) + \frac{e^{-ikr}}{4\pi r} \left( ik + \frac{1}{r} \right) \cos \beta \vec{p}(X)) dA(X) \quad (9)$$

$$\text{With, } C(Y) = \begin{cases} 1, Y \in D \\ 1 - \int_A \frac{\cos \beta}{4\pi r^2} dA, Y \in A \\ 0, Y \notin (D \cup A) \end{cases}$$

Where,  $\beta$  is the angle between normal vector of  $X$  point on the structure surface and radius vector  $r$ ,  $D$  is the fluid domain.

There are  $M$  elements and  $N$  nodes on the boundary by dividing the surface  $A$  of the vibrating structure.  $L$  is the nodes of each element. Suppose that the local coordinates of any point on the unit  $(x, y, z)$  is  $(\xi, \eta)$ . We get,

$$\begin{cases} \vec{p}(x, y, z) = \sum_{i=1}^L N_i(\xi, \eta) \vec{p}_i \\ \vec{v}_n(x, y, z) = \sum_{i=1}^L N_i(\xi, \eta) \vec{v}_{ni} \end{cases} \quad (10)$$

Where,  $N_i(\xi, \eta)$  is interpolating shape function. Each node on the boundary is used as the source in turn, the formula of (11) can be obtained by discretizing the Helmholtz integral equation.

$$Q\vec{p} = P\vec{v}_n \quad (11)$$

$Q$  and  $P$  are all symmetric plural full rank matrix, which are functions of excitation frequency and are related to the surface shape, size and interpolating shape function of the structure.  $\vec{p}$  and  $\vec{v}_n$  are column vectors at  $N$  dimensions.

$$\vec{p} = Z\vec{v}_n \quad (12)$$

Where,  $Z = Q^{-1}P$ ,  $Z$  is the vibration structure acoustic impedance matrix, any unit  $z_{ij}$  represents the contribution of the unit velocity at the node  $j$  to the sound pressure at the node  $i$ .

With the acquisition of  $\vec{p}$  and  $\vec{v}_n$ , the radiated sound pressure at any point in the sound field can be obtained by the Helmholtz integral equation ( $Y \in D$ ),

$$\vec{p}(Y) = q^T \vec{p} + k^T \vec{v}_n \tag{13}$$

Where,  $q$  and  $k$  are interpolation shape function column vectors related to the shape of structure surface as well as the location of  $Y$ , determined by Eq. (9).

For the non-closed elevated box bridge structure, the sound pressure at any point in the sound field can be obtained by calculating the difference between Helmholtz integral equations on both sides of the boundary surface,

$$\vec{p}(Y) = \int_A \left( \frac{e^{-ikr}}{4\pi r} \Delta \vec{v}(X) + \frac{e^{-ikr}}{4\pi r} \left( ik + \frac{1}{r} \right) \cos \beta \Delta \vec{p}(X) \right) dA(X) \tag{14}$$

Where,  $\Delta \vec{v}(X)$  is the speed difference of  $X$  point on both sides of the surface,  $\Delta \vec{p}(X)$  is the sound pressure difference of  $X$  point on both sides of the surface.

Being respectively expressed as

$$\begin{cases} \Delta \vec{v}(X) = -i\rho_0\omega(\vec{v}_{n1}(X) - \vec{v}_{n2}(X)) \\ \Delta \vec{p}(X) = \vec{p}_1(X) - \vec{p}_2(X) \end{cases} \tag{15}$$

Where,  $\vec{p}_1(X)$  and  $\vec{p}_2(X)$  are pressure of  $X$  point on both sides of the structural surface;  $\vec{v}_{n1}(X)$  and  $\vec{v}_{n2}(X)$  indicate normal vibration speed of  $X$  point on both sides of the structure surface.

When the structural surface is separated by the boundary elements, the difference of the velocity and the sound pressure of the nodes can be expressed by

$$\begin{Bmatrix} \Delta \vec{v}(X) \\ \Delta \vec{p}(X) \end{Bmatrix} = C^{-1} F \tag{16}$$

Where,  $C$  is a symmetric-complex full rank matrix which is related to the shape, size and interpolated shape of the structural surface and is a function of the exciting frequency.  $F$  is external excitation vector depending on the structural surface vibration velocity.

Sound pressure of any point outside the structural surface  $\vec{p}$  can be obtained by (14).

$$\vec{p}(Y) = B \begin{Bmatrix} \Delta \vec{v}(X) \\ \Delta \vec{p}(X) \end{Bmatrix} = BC^{-1} F \tag{17}$$

Where,  $\vec{p}(Y)$  is the sound pressure of any observation point,  $B$  is the interpolation matrix determined by Eq. (14).

### 3 Dynamic Analysis of the Box Girder Bridge

When a train moves through the elevated box girder bridge at a velocity of 200 km/h, the train axial load is 191.1kN, corresponding to  $p_1-p_4$  in Fig. 1, the parameters used to confirm the wheel location are  $d_1 = 2.5$  m,  $d_2 = 17.37$  m, respectively, as shown in Fig. 1. The simply supported concrete single box single cell elevated box bridge, which is commonly used in high-speed railway, is adopted for the case studies. The total length of the track slab is 32 m and the thickness of the slab is 3 m, the thickness of the deck plate, the web and the bottom plate is 0.315 m, 0.480 m and 0.300 m, respectively. The bridge uses CRTS type I double-track slab ballastless structure; the length, width and thickness of track plate is 4.93 m, 2.4 m and 0.2 m, respectively, the rail type is 60 kg/m. other specific parameters are shown in Table 1.

**Table 1.** Track and bridge dynamics parameters

Dynamic parameters	Parameter values	Dynamic parameters	Parameter values
Elastic modulus of rail/(N·m <sup>-2</sup> )	$2.1 \times 10^{11}$	Adjust the layer stiffness under the track plate/(N·m <sup>-1</sup> )	$9.375 \times 10^9$
Inverse moment of rail/(m <sup>4</sup> )	$3.215 \times 10^{-5}$	Adjust the layer damping under the track plate/(N·s·m <sup>-1</sup> )	$7.5 \times 10^5$
Poisson's ratio of rail	0.3	Elastic modulus of base/(N·m <sup>-2</sup> )	$3.3 \times 10^{10}$
Rail line density/(kg·m <sup>-1</sup> )	60.64	Poisson ratio of Base	0.2
Rigidity of cushion under the track/(N·m <sup>-1</sup> )	$4 \times 10^7$	Density of Base/(kg·m <sup>-3</sup> )	2500
Damping of cushion under the track/(N·s·m <sup>-1</sup> )	$2.2656 \times 10^4$	Elastic modulus of bridge/(N·m <sup>-2</sup> )	$3.8 \times 10^{10}$
Elastic modulus of track plate/(N·m <sup>-2</sup> )	$3.6 \times 10^{10}$	Poisson ratio of bridge	0.25
Poisson ratio of track plate	0.2	Density of bridge/(kg·m <sup>-3</sup> )	2500
Track plate density/(kg·m <sup>-3</sup> )	2500		

Figure 2 shows the time-varying acceleration and spectrum of the various parts of the elevated box bridge across the center.

It can be observed from Fig. 2 that the vibration of the deck plate is the largest compared to the web and the bottom plate. From the spectrum shown in Fig. 2(b), the vibration frequency is mainly concentrated at the frequency range of 0–300 Hz, most of the peaks appear at 10–160 Hz in the low frequency band.

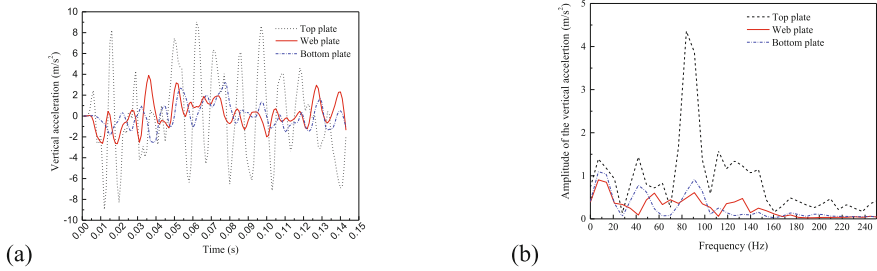


**Fig. 2.** Acceleration response of bridge structure vibration at mid span (a. Vertical acceleration time histogram, b. Vertical acceleration spectrum)

### 4 Sound Radiation Analysis

The dynamic responses of the box bridge structures are used as the acoustic boundary condition to calculate the influence of the box bridge structure on the sound field of the surrounding space. Assuming that the height of bridge pier is 20 m, the field points are selected, as shown in Fig. 4(a). This paper uses linear weighted sound pressure levels in the analytical process.

Both Figs. 3 and 4(b)(c)(d) show the two-dimensional sound field distribution and the sound pressure level (SPL) of the selected field points. These figures show that the elevated box bridge under the train moving axial load can produce large structural noise, which is more intensive at the upper and bottom of the structures. As the train runs on the single line, the sound field distribution on both sides of the bridge is not symmetrical. When the frequency is low, the directivity of the sound field is strong, and the radiation noise decreases with the increase of the frequency. The SPLs of the field points of the bottom of the bridge is the largest, which increases with the increase of the ground distance; when the distance is closer to the box bridge structure at the center frequency of 80–100 Hz, the SPLs is obviously higher than other field points; The SPLs of the transverse field points decreases with the increase of the distance, and the SPL of the near field points of the box bridge is slightly higher than that of the bottom. For the far field region in the vertical direction, the structural noise changes are more complicated.



**Fig. 3.** Two-dimensional sound field distribution cloud at mid span (10 Hz-left, 118 Hz-right)



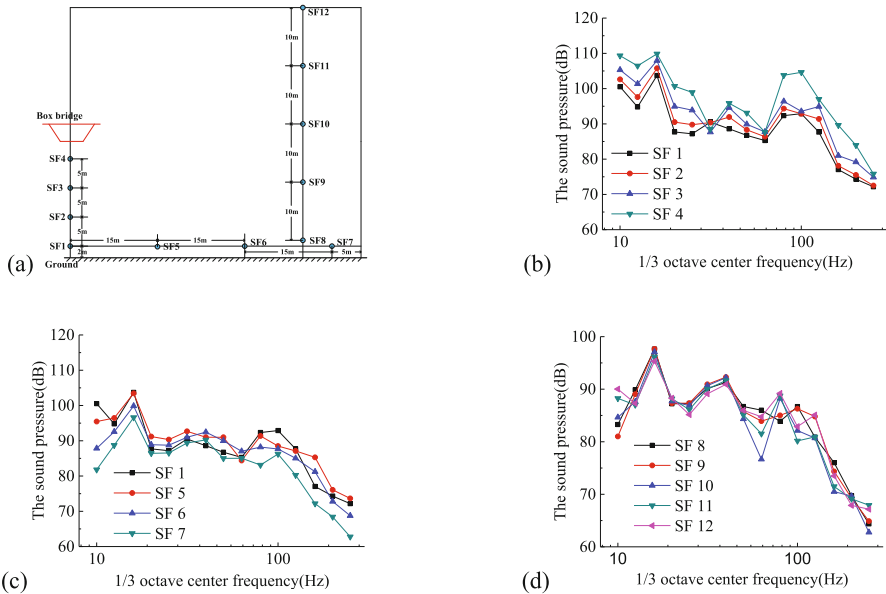


**Fig. 4.** Field points velocity SPL spectrum curve at 200 km/h (a. Field points distribution, b. SPL at the bottom, c. SPL of transverse, d. SPL in far-field)

## 5 Conclusions

- (1) The plate-shell element can reflect the whole and local vibration characteristics of the box bridge well, and under the effect of moving axial load, the vibration frequencies of box bridge structure concentrate in 0–300 Hz and the main peaks are in 10–160 Hz.
- (2) The finite element-boundary element method can effectively calculate the low frequency noise radiation of box bridge induced by the moving axial load; most of the structural noise induced by moving axial load is below the audible range that is greatly harmful to human body, therefore, it must be dealt with seriously;

**Acknowledgment.** This research was supported by the Open Project of State Key Laboratory of Traction Power, Southwest Jiaotong University (TPL1604); Gansu Province Natural Science Foundation of China (1606RJZA014); Young Fund of Lanzhou Jiaotong University (2015025).

## References

1. Zhai, W.M., Xia, H.: Train-Track-Bridge Dynamic Interaction: Theory and Engineering Application. Science Press, Beijing (2011)
2. Zhai, W.M., Cai, C.B., et al.: Mechanism and model of high-speed train-track-bridge dynamic interaction. China Civil Eng. J. **38**(11), 132–137 (2005)

3. Cai, C.B., Zhai, W.M., et al.: Dynamics simulation of interactions between high-speed train and slab track laid on bridge. *China Railway Sci.* **25**(5), 57–60 (2004)
4. He, Z.X., Zhai, W.M., Yang, X.W., et al.: Moving train axle-load induced ground vibration and mitigation. *J. Rail Way Sci. Eng.* **4**(5), 73–77 (2007)
5. He, Z.X., Zhai, W.M., Wang, S.Z., et al.: Semi-analytical study on ground vibration induced by railway traffics with axle loads. *J. Vib. Shock* **26**(12), 1–5 (2007)
6. Janssens, M.H.A., Thompson, D.J.: A calculation model for the noise from steel railway bridge. *J. Sound Vib.* **193**(1), 295–305 (1996)
7. Bewes, O.G., Thompson, D.J., Jones, C.J.C., et al.: Calculation of noise from railway bridge and viaducts: experimental validation of a rapid calculation mode. *J. Sound Vib.* **293**(3–5), 933–943 (2006)
8. Thompson D.J., Jones C.J.C., Bewes O.G.: *Software for Predicting the Noise of Railway Bridge and Elevated Structures-Version 2.0*. Southampton: Institute of Sound and Vibration Research (2005)
9. Li, X.Z., Zhang, X., Liu, Q.M., et al.: Prediction of structure-borne noise of high-speed railway bridges in whole frequency bands (Part I): theoretical model. *J. China Railway Soc.* **35**(1), 101–107 (2013)
10. Zhang, X., Li, X.Z., Liu, Q.M.: Prediction of structure-borne noise of high-speed railway bridges in whole frequency bands (Parts II): field test verification. *J. China Railway Soc.* **35**(2), 87–92 (2013)
11. Zhang, X., Li, X.Z., et al.: Sound radiation characteristics of 32 m simply supported concrete box girder applied in high-speed railway. *J. China Railway Soc.* **34**(7), 96–102 (2012)
12. Augusztinovicz, F., Marki, F., Nagy, A.B., et al.: Derivation of train track isolation requirement for a steel road bridge based on vibro-acoustic analyses. *J. Sound Vib.* **293**(3/4/5), 953–964 (2006)
13. Ouelaa, N., Rezaiguia, A., Laulagnet, B.: Vibro-acoustic modeling of a railway bridge crossed by a train. *Appl. Acoust.* **67**(5), 461–475 (2006)
14. Song, L.M., Sun, S.G.: Noise predicting based on viaduct structure of railway. *J. Beijing Jiaotong Univ.* **33**(4), 42–45 (2009)
15. Ngai, K.W., Ng, C.F.: Structure-borne noise and vibration of concrete box structure and rail viaduct. *J. Sound Vib.* **255**(2), 281–297 (2002)
16. Li, Q., Xu, Y.L., Wu, D.J.: Concrete bridge-borne low-frequency noise simulation based on train-track-bridge dynamic interaction. *J. Sound Vib.* **331**(10), 2457–2470 (2012)